Recovering more classes than available bands for sets of mixed pixels in satellite images

M. Faraklioti [a] M. Petrou [a]

[a] *School of Electronic Engineering, Information Technology and Mathematics, University of Surrey, Guildford, Surrey, GU2 5XH, UK*

Abstract

The classification of sets of mixed pixels can be accomplished by making use of the relationship of higher order moments of the distributions of the pure and mixed classes. As a consequence, the number of equations relating the means of the distributions can be augmented, providing a number of linear equations larger than the number of available sensor bands. Thus, the important advantage the method offers and makes it unique is the fact that more classes than available bands can be identified. The capabilities and limitations of the method are assessed first by the use of simulated data that closely imitate real data, and also by real data from Landsat images.

Key words: Mixed Pixels; Subpixel Classification; Multispectral Images

1 Introduction

Recently, remote multispectral data collection and automatic processing techniques have been proven to be very useful tools for many applications in the field of Earth surveys. For certain applications however, limits in the spatial resolution of satellite sensors and variation in ground surface cover, restrict the usefulness of the remotely sensed multispectral data resulting in the presence of mixed pixels. In this case, the observed spectral signature of pixels is the result of the reflecting properties of a number of surface materials constituting the area of the pixel. There are three main approaches that have been developed to deal with the pixel classification problem: *Calculation of indices* [6],[12],[8], *Statistical methods of image classification* [7], [5] and *Spectral mixture analysis*. The first two methods result in the production of large thematic maps which can often be poor representation of reality. Therefore, a spectral mixture analysis approach is usually followed, which attempts to model how the area on the ground which corresponds to each pixel is divided up among

different cover types given the multispectral observations. Among various mixing models, the linear mixing model has been most commonly used in many previous studies of mixing in remote sensing [9],[3],[10],[2],[4]. Under the assumption that each photon that reaches the sensor has interacted with only one cover type, the spectral reflectance of each mixed pixel in any wavelength, can be considered as a linear combination of the spectral reflectances of the components that constitute the mixture, weighted by their relative proportions in the mixture. The spectra of the pure classes [11] are used as training data necessary to perform the unmixing.
In this paper we investigate the ability to recover more classes than available bands of a recently proposed method[1]. The method is appropriate for the classification of whole regions of mixed pixels in a scene assuming that they possess identical composition. The model is an extension of the linear mixing model: The spectral reflectance of a mixed pixel in a spectral band is assumed to be the linear superposition of the reflectances of the classes present in the pixel, weighted by the fraction with which they contribute to the pixel. To solve such a system of equations for the weights it is necessary to have as many bands (equations) as unknowns (pure classes). For the case of sets of mixed pixels for which we wish to determine the fractions of the pure classes present in them, each set may be considered as an ensemble of instantiations of the same random variable. Then the set of linear equations, that relate the spectral reflectances of the pure and mixed classes, can be supplemented by extra equations that relate the moments of the mixed and the pure pixel sets. Bosdogianni et.al.[1] used this to add robustness to the set of equations. However, if we have extra equations, we may be able to solve systems for more unknowns, at the expense of the added robustness. This paper investigates theoretically this aspect of the proposed model, in particular with respect to the accuracy it can achieve, its robustness and its breaking points. The investigation is done with the help of simulated sets of pixels distributed either according to the normal distribution, or according to the uniform distribution, with parameters that closely follow distributions of real data. Finally, the method is applied to some real data as well.

2 More components than bands

The set of equations for the mean values of the spectral reflectances for mixed and pure classes according to the linear mixing model is:

$$\bar{w}_i = a\bar{x}_i + b\bar{y}_i + c\bar{z}_i + d\bar{v}_i \tag{1}$$

where $\bar{w}_i$ represents the mean value of the known spectral reflectance of the mixed pixel distribution in band i, $\bar{x}_i, \bar{y}_i, \bar{z}_i$ and $\bar{v}_i$ represent the mean values

of the known spectral reflectances of the four possible cover components in the mixed pixel, and a, b, c and d represent the proportions of the four components in the set of mixed pixels. Considering only two bands ($i = 2$), equation (1) represents a set of 2 equations, one for each band. Adding the sum-to-one constraint ($a + b + c + d = 1$), we finally end up with a total number of three equations with four unknowns (the four fractions of the components). This set of equations is supplemented by the equations that relate the second order moments of the distributions of the pure and mixed classes:

$$covw_i w_j = a^2 covx_i x_j + b^2 covy_i y_j + c^2 covz_i z_j + d^2 covv_i v_j \tag{2}$$

where $covw_i w_j, covx_i x_j, covy_i y_j, covz_i z_j, covv_i v_j$ represent the covariances of mixed and pure distributions respectively between bands i and $j (i, j = 1, 2)$. Equation (2) adds to the problem 3 more equations. As a result, 6 equations exist in total, with 4 unknowns. This is the case that inversion can be performed by the Constrained Least Square Error method. The proportions a, b, c and d can be calculated subject to the constraints that they must be non-negative and add up to one. Our purpose is to determine the class composition of a hypothesised test site using the observed spectral response of the mixed pixels and the training data that describe the pure classes. The problem will be solved by exhaustive search of all possible combinations of a, b, c and d to find the one that minimises the total square error. However, the reliability of equations (2) is not the same as the reliability of equations (1): second order moments of sets of samples are less reliably calculated than first order moments. So, in the definition of the total square error, the errors arising from the different equations are weighted inversely proportionally to the standard error with which an indicative quantity of one of the variables can be calculated. As such indicative quantities we use the quantities that refer to the set of mixed pixels, i.e. we use the standard error with which the statistics of mixed pixels are computed. Therefore, the total error we wish to minimize is:

$$\begin{aligned} E_{TOTAL} = & \sum_{i=1}^{2} \frac{N}{varw_i} (\bar{w}_i - a\bar{x}_i - b\bar{y}_i - c\bar{z}_i - d\bar{v}_i)^2 + \\ & \sum_{i=1}^{2} \sum_{j=1}^{2} \frac{N}{2(covw_{ij})^2} (covw_i w_j - a^2 covx_i x_j - \\ & b^2 covy_i y_j - c^2 covz_i z_j - d^2 covv_i v_j)^2 \end{aligned} \tag{3}$$

where N is the number of mixed pixels. To evaluate the performance of the model, the coverage proportions of the mixed pixels used are assumed to be known in advance, by ground inspection, so that the results of the method can be compared with the real proportions. It was assumed that the measured mixing proportions were: $a = 10\%, b = 20\%, c = 30\%, d = 40\%$ for four

hypothetical classes X,Y,Z and V. For training, artificially created data were used, presumed to be image training data extracted from a specific image. An algorithm was developed to implement the above equation which exhaustively searches all possible combinations of the proportions and returns the one that minimises the square error. Accuracy of $\pm 1\%$ for the percentage coverage was considered to be enough for performing the exhaustive search. A series of test runs were made to determine the capabilities and limitations of the chosen model. We were especially interested in the accuracy of estimation of the proportions and the effect on it of the characteristics and the number of sample points used. The following section gives the results of the simulations.

3 Simulation results

3.1 Normally distributed data

As a first stage of assessing the model, normally distributed training data were chosen to be used. In general, this type of distribution is very commonly used in remote sensing applications. The simulated data that represent the pure and mixed classes were created so as to approximate as much as possible, real data found in some remote sensing applications[1]. The means and the covariance matrices of the sets representing the pure classes were chosen as shown in Table 1. The mean and covariance matrix of the mixed class were computed from them using the proportions we chose.

Table 1
Statistical characteristics of the pure and mixed classes normally distributed

Class	Mean (band 1)	Mean (band 2)	Variance (band 1)	Variance (band 2)	Covariance (bands 1,2)
X	10	25	15	25	12
Y	40	40	25	7	5
Z	25	20	12	20	10
V	20	40	18	15	8
W	24.5	32.5	5.11	4.73	2.5

Using the values of Table 1, five two-dimensional distributions for the five components were created by random number generation. For evaluating the applicability of our model the effect of the size of the pure and mixed data set on the proportion estimation was examined. So, in a first series of experiments the mixed class was represented by 500 samples, but the pure classes,

by numbers varying from 200 to 8000. For each combination of values 100 different sets of pixel sets were drawn. For each set of pixel sets the proportions were estimated as described above and the percentage error was calculated for each variable. Then, these errors from the 100 sets of pixel sets were used to calculate the mean and the standard deviation of the expected percentage error. The results are shown in Figure 1.

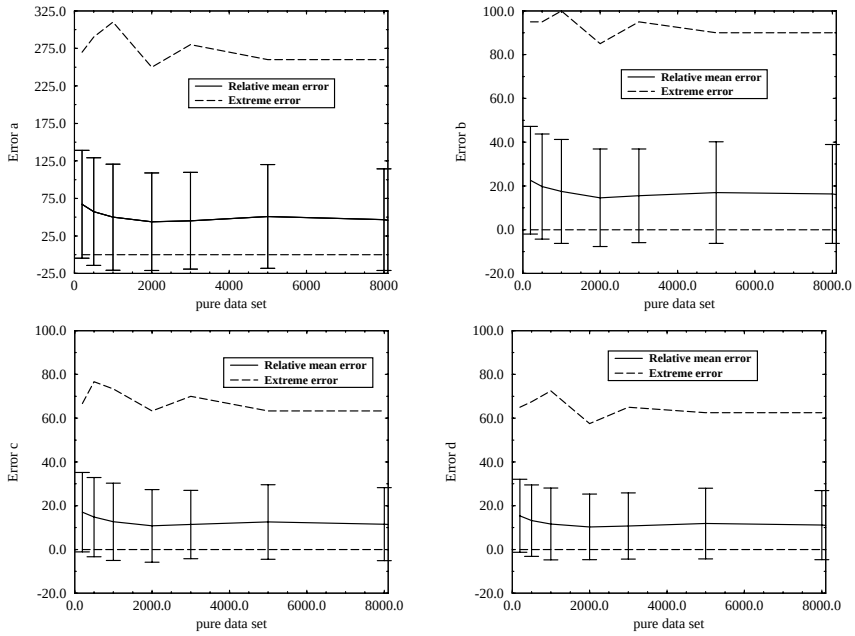

Fig. 1. Mean relative error of proportion estimation over 100 experiments versus the size of the pure data set for normal distributions for 500 points of mixed data. The true values of the proportions are: $a = 10\%, b = 20\%, c = 30\%$ and $d = 40\%$. The dashed lines indicate the minimum and maximum errors and the bars the standard deviation of each distribution of errors.

In the second series of experiments, the pure classes were represented by 500 samples each and the mixed class by 200 up to 8000. Again, 100 different sets of sample sets were created for each combination of populations, and statistics over the errors of the method were compiled. These results are shown in Figure 2. The error bars represent the standard deviation of the error distribution for each set. The extreme errors represent the highest and lowest values of errors observed in every test. It is obvious that the errors obtained for the case of 500 points proved to exhibit quite high values. Thus, to overcome the problem of undersampling, we performed both the previous experiments using 10,000 points to represent the mixed class in the first experiment and the pure classes in the second. The results of the simulations in Figures 3,4 show a great improvement in the performance of the method. It seems that 3000 points of pure or mixed data is enough to provide an insignificant error. It may also be noted that the smallest proportions are estimated with less accuracy than the largest ones. Furthermore, it seems important that a sufficient sample size of mixed pixels is available since the model performs better in the case when the

mixed class is better defined than the pure classes.

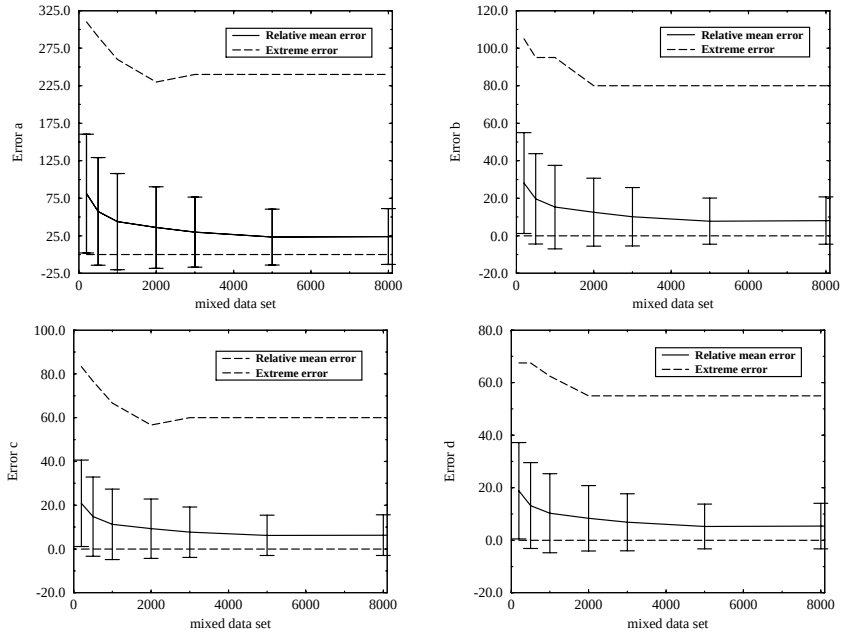

Fig. 2. Mean relative error of proportion estimation over 100 experiments versus the size of the mixed data set for normal distributions for 500 points of pure data.

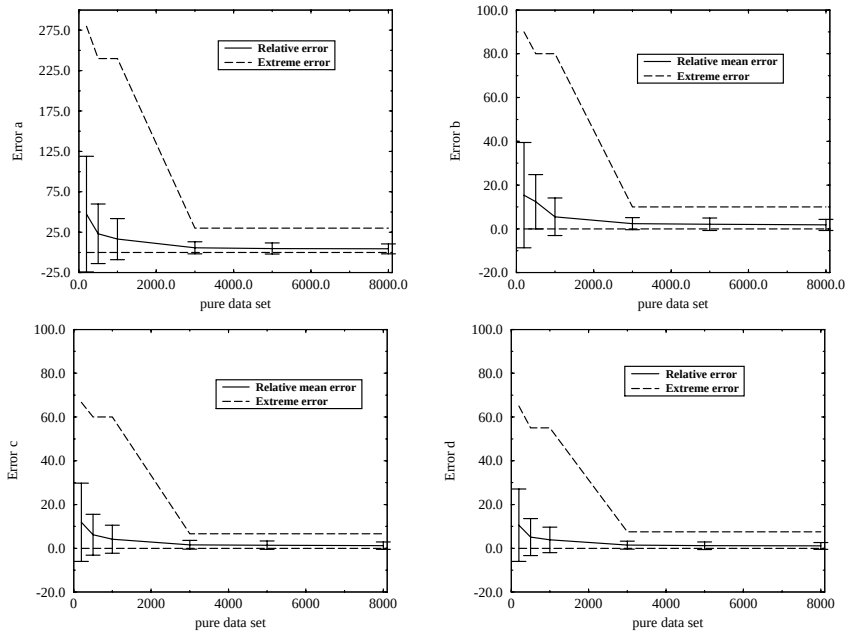

Fig. 3. Mean relative error of proportion estimation over 100 experiments versus the size of the pure data set for normal distributions for 10000 points of mixed data.

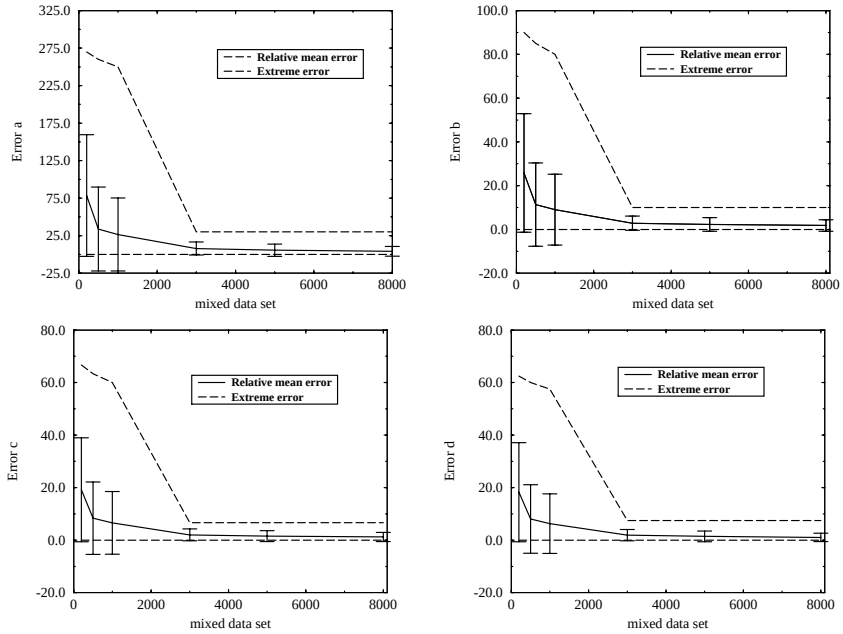

Fig. 4. Mean relative error of proportion estimation over 100 experiments versus the size of the mixed data set for normal distributions for 10000 points of pure data.The true values of the proportions are: $a = 10\%, b = 20\%, c = 30\%$ and $d = 40\%$. The dashed lines indicate the minimum and maximum errors and the bars the standard deviation of each distribution of errors.

3.2 Uniformly distributed data

Table 2 gives the statistics of the uniform distributions of sample points created. To create one such set, a large number of sample points was created over a square area which was subsequently clipped to have a polygonal shape that somehow resembled the shape of the distributions of the real data in [1]. Each mixed pixel was generated as a linear combination of individual pure pixels which were discarded from the pure distributions. Figures 5, 6, 7 and 8 show

Table 2
Statistical characteristics of the pure and mixed classes uniformly distributed

Class	Mean (band 1)	Mean (band 2)	Variance (band 1)	Variance (band 2)
X	8.1	12.6	21.5	27.8
Y	38.4	43.6	37.6	42.8
Z	23.0	27.3	16.6	23.5
V	16.0	23.2	36.8	41.7

the results obtained for these distributions. All experiments were contacted in

the same format as the experiments for the Gaussian distributions. The errors here seem to be less dependent on the number of samples and smaller than in the case of Gaussian distributions.

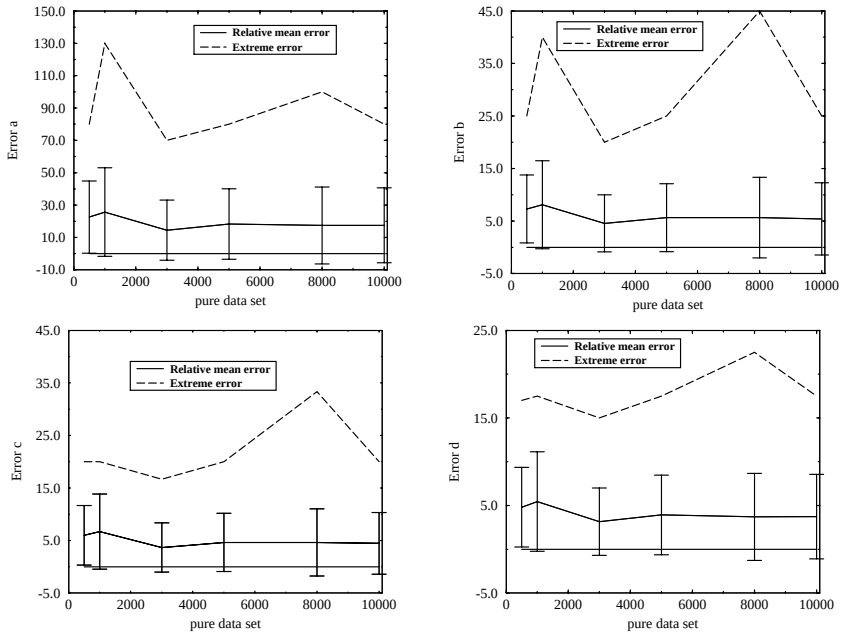

Fig. 5. Mean relative error of proportion estimation over 100 experiments versus the size of the pure data set for uniform distributions for 500 points of mixed data.

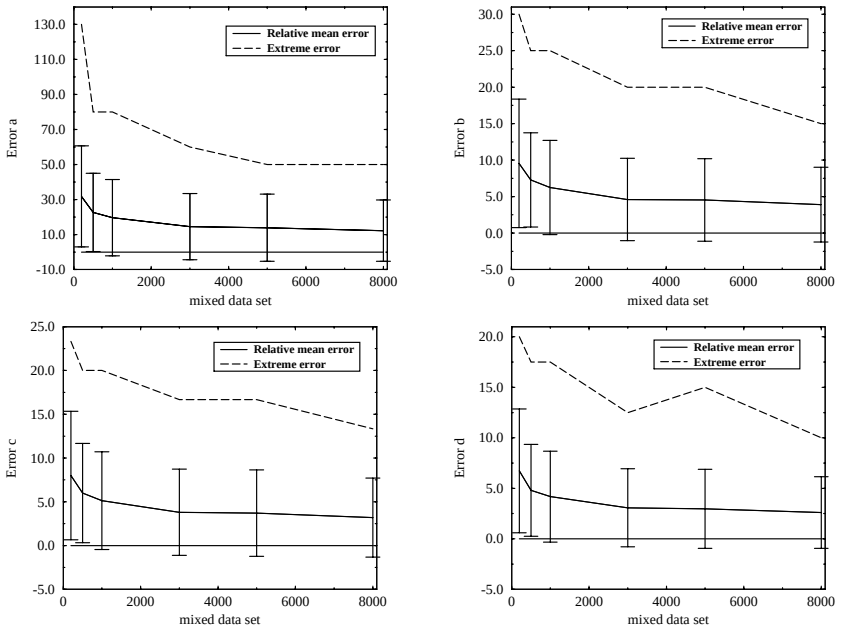

Fig. 6. Mean relative error of proportion estimation over 100 experiments versus the size of the mixed data set for uniform distributions for 500 points of pure data.The true values of the proportions are: $a = 10\%, b = 20\%, c = 30\%$ and $d = 40\%$. The dashed lines indicate the minimum and maximum errors and the bars the standard deviation of each distribution of errors.

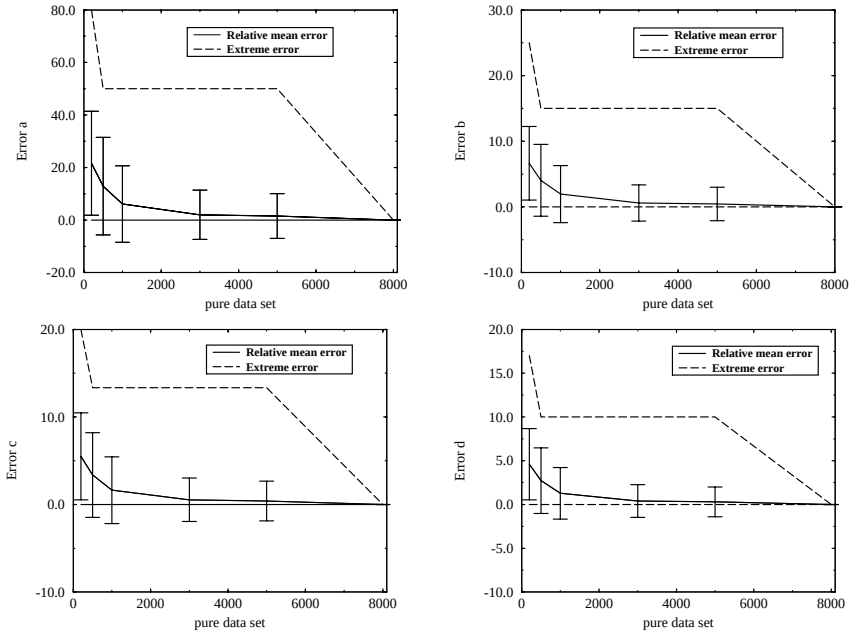

Fig. 7. Mean relative error of proportion estimation over 100 experiments versus the size of the pure data set for uniform distributions for 10000 points of mixed data.

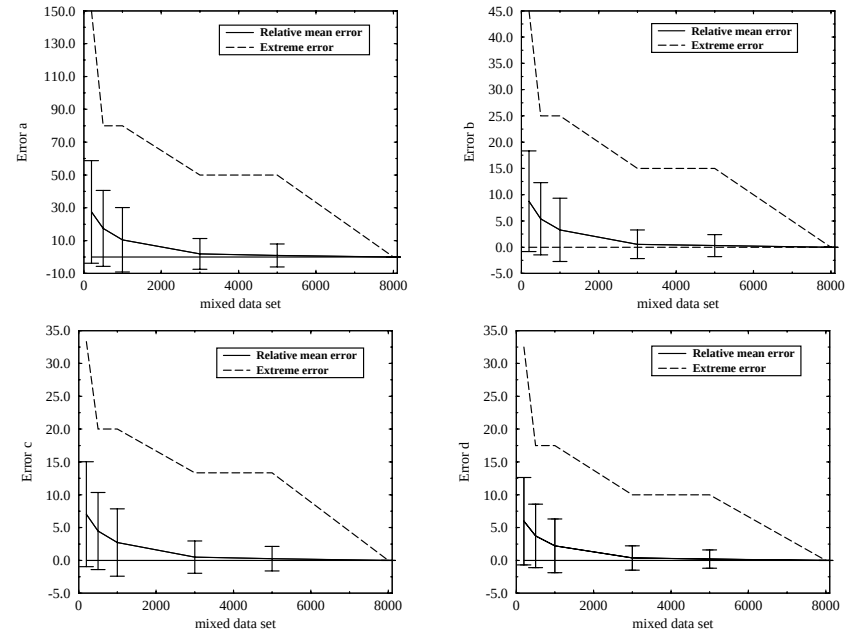

Fig. 8. Mean relative error of proportion estimation over 100 experiments versus the size of the mixed data set for uniform distributions for 10000 points of pure data.The true values of the proportions are: $a = 10\%, b = 20\%, c = 30\%$ and $d = 40\%$. The dashed lines indicate the minimum and maximum errors and the bars the standard deviation of each distribution of errors.

4 Application to real satellite imagery

To evaluate the method with real satellite data, we used the data from Landsat TM image depicting various burned forest sites in Greece, for which ground data are available. The data had been collected by NARF, (Institute of Mediterranean Forest Ecosystem-National Agricultural research foundation of Greece) as part of a project concerned with monitoring forest regeneration from space. Four ground cover classes had been identified in each site by ground inspection: aleppo pine, maquis, phrygana and bare soil. Although all TM bands are available for the image that covers this area, we shall use only the values of red and infrared bands to test our approach: We shall try to identify four cover classes from only two spectral bands.

For our method, training data are necessary, representative of the four pure classes. The terrain under consideration is characterised by great subpixel variability due to sparse vegetation. As a result, it is impossible to extract sets of pixels representing the pure classes from the image itself. Therefore, the statistics (mean values and covariance matrices) of the pure classes had to be derived from the use of mixed sites with known composition [1].

If $i = 1, .., n$ where n is the number of the used spectral bands, then our problem can be described by the equation:

$$\bar{w}_{k,i} = a_k \bar{x}_i + b_k \bar{y}_i + c_k \bar{z}_i + d_k \bar{v}_i \tag{4}$$

where: $k = 1, .., m$ and m is the number of mixed sites used for training ($m \geq 4$). This can also be expressed in a matrix form as:

$$W = PX \tag{5}$$

where W is an $(nm \times 1)$ matrix containing the mean values of the m sites in n bands, P is an $(mn \times 4n)$ matrix containing the proportions of the pure classes, which are the same in all bands that refer to the same sites and X is a $(4n \times 1)$ matrix containing the unknown mean values of the pure classes in the n bands. Thus, equation (5) represents an overdetermined system of mn equations for $4n$ unknowns. The system was solved for the vector of the mean values, X, by taking the pseudoinverse of matrix P. A similar overdetermined system of linear equations in a^2, b^2, c^2 and d^2 was solved for the estimation of the elements of the covariance matrices of the pure classes.

There were 23 mixed sites available for training and 8 mixed sites for testing. Each of these sites consisted of about 30 to 150 mixed pixels.

Initially, all 23 sites were used for training. After the solution of (5), the mixing

proportions of the training sites were derived using the estimated spectral characteristics of the pure classes. Only the proportions of 13 out of the 23 sites could be recovered to a satisfactory degree. This shows that there were serious inconsistencies with the training data. The 10 sites that seemed to be inconsistent with the rest were omitted, and system (5) was solved again for the remaining 13 sites only. The characteristics of the pure classes computed this way from the remaining sites are given in Table 3.

Table 3
Statistical characteristics of the pure classes as estimated from 13 sites.

Class	Mean (band 1)	Mean (band 2)	Variance (band 1)	Variance (band 2)	Covariance (bands 1,2)
S	55.35	56.91	87.15	77.72	73.12
AP	23.37	46.12	16.44	4.60	-5.05
M	20.15	50.28	51.01	99.47	16.60
P	13.7	24.88	21.33	62.49	37.27

In this table, S stands for the soil, AP for Aleppo Pine, M for maquis and P for Phrygana.

Table 4 shows the results of estimating the mixing proportions of the 13 training sites. Two criteria used to judge success or failure were : According to the first criterion, the classification was considered successful (hit) if the dominant class only was correctly identified, otherwise, it was considered a "miss". According to the second criterion, the "hit" condition was accepted if the dominant class was identified within an accuracy of $\pm 15\%$. Under the heading "Ground", the proportions of each class are given, as obtained from ground inspection. Under the heading "Method", the results as obtained from the method discussed are provided. According to the first criterion all 13 sites were classified correctly, while according to the second criterion, 7 out of the 13 sites were classified correctly.

Next the model was applied to the 8 sites that did not contribute to the training process. The classification results were obtained by using the statistics of pure classes estimated by the training procedure and are shown in Table 5.

Table 4
Comparison of the classification results of our model with the ground truth data of 13 training sites.

Site	Ground				Method				Results	Results
num	S	AP	M	P	S	AP	M	P	criterion1	criterion2
1	20	30	0	50	31	0	25	44	HIT	HIT
2	15	30	0	55	14	40	0	46	HIT	MISS
3	35	20	10	35	46	0	9	45	HIT	MISS
4	55	15	10	20	53	29	0	18	HIT	HIT
5	10	70	0	20	3	57	13	27	HIT	MISS
6	15	45	30	10	21	65	0	14	HIT	MISS
7	20	60	0	20	14	65	21	0	HIT	HIT
8	0	75	0	25	0	64	8	28	HIT	HIT
9	5	55	5	35	7	42	30	21	HIT	MISS
10	15	0	65	20	25	8	51	16	HIT	MISS
11	30	0	40	30	2	33	37	28	HIT	HIT
12	5	35	0	60	0	35	0	65	HIT	HIT
13	5	0	55	40	13	4	56	27	HIT	HIT

Table 5
Comparison of the classification results of our model with the ground truth data of 8 test sites.

Site	Ground				Method				Results	Results
num	S	AP	M	P	S	AP	M	P	criterion1	criterion2
1	5	0	50	45	0	25	45	30	HIT	HIT
2	0	0	85	15	8	0	57	35	HIT	MISS
3	15	65	0	20	42	58	0	0	HIT	HIT
4	10	50	0	40	33	57	1	9	HIT	HIT
5	35	35	5	25	3	58	4	8	HIT	MISS
6	30	50	5	15	13	42	35	10	HIT	MISS
7	60	10	0	25	55	4	31	10	HIT	HIT
8	5	55	10	30	6	44	0	50	MISS	MISS

As it can be seen, the model performs very well in identifying correctly the dominant class in the scene. It also showed ability in classifying the dominant class within acceptable limits, in half of the cases.

5 Conclusions

Real data are neither Gaussianly distributed nor uniformly. Real distributions are usually something in between these two cases. It was shown that in general 2000-3000 sample points are necessary for each class, for an acceptable level of error (error of the order of $5-10\%$). Such error levels are compatible with the errors in ground data [1] and one should not expect to do much better than that using satellite images. Having a few thousand pixels per class is equivalent to having regions of size 30×30 to 100×100 pixels to classify. For Landsat images with $30m$ resolution this corresponds to $1km^2$ to $9km^2$, for SPOT data to $0.1km^2$ regions of uniform coverage on the ground. This is not unrealistic. In particular, data collected from sensors with even higher resolution will be even more appropriate for this type of approach to spectral unmixing. In general, it is possible to use this approach even with coarser data, such as the NASA MODIS and ENVISAT MERIS instruments, provided that each site can be represented by a large enough number of pixels for reliability. On the other hand, if the intraclass variability is not as severe as that we used here, one may be able to obtain reliable results with even fewer pixels per class. The results, from applying the method to simulated data, show that it presents high accuracy in identifying the primary class, and relatively low accuracy in small proportion estimation.

At a first glance, the results of the experiments with real data appear poor. However, as concluded above, for reliable results, one needs 2000-3000 points to represent each class. The real data we had, used 30-150 points for each class! One can see from figures 1-4 that for such levels of undersampling one expects totally unreliable results. The fact that the method was able to identify reasonably well the dominant class is a true success.

It should also be noted that the method was quite easy to implement and of low computational cost.

References

[1] P. Bosdogianni, M. Petrou, and J. Kittler. Mixture models with higher order moments. *IEEE Transactions on Geoscience and Remote Sensing*, 35:341–353, 1997.

[2] A.M. Cross, J.J. Settle, N.A. Drake, and R.T.M. Paivinen. Subpixel measurement of tropical forest cover using AVHRR data. *International Journal of Remote Sensing*, 12:1119–1129, 1991.

[3] G.M. Foody and D.P. Cox. Sub-pixel land cover composition estimation using a linear mixture model and fuzzy membership functions. *International Journal of Remote Sensing*, 15:619–631, 1994.

[4] C.A. Hlavka and M.A. Spanner. Unmixing AVHRR imagery to assess clearcuts and forest regrowth in oregon. *IEEE Transactions on Geoscience and Remote Sensing*, 33:788–795, 1995.

[5] H.M. Horwitz, R.F. Nalepka, P.D. Hyde, and J.P. Morganstern. Estimating the proportion of objects within a single resolution element of a multispectral scanner. *University of Michigan, Ann Arbor, Michigan, NASA Contract NAS-9-9784*, 1971.

[6] C.O. Justice, J.R.G. Townshend, B.N. Holben, and C.J. Tucker. Analysis of the phenology of global vegetation using meteorological satellite data. *International Journal of Remote Sensing*, 6:1271–1318, 1985.

[7] S.E. Marsh, P. Switzer, W.S. Kowalik, and R.J.P. Lyon. Resolving the percentage of component terrains within single resolution element. *Photogrammetric Engineering and Remote Sensing*, 46:1079–1086, 1980.

[8] A.J. Richardson and C.L. Wiegand. Distinguishing vegetation from soil background information. *Photogrammetric Engineering and Remote Sensing*, 43:1541–1552, 1977.

[9] J.J. Settle and N.A. Drake. Linear mixing and the estimation of ground cover proportions. *International Journal of Remote Sensing*, 14:1159–1177, 1993.

[10] Y.E. Shimabukuro and J.A. Smith. The least-squares mixing models to generate fraction images derived from remote sensing multispectral data. *IEEE Transactions on Geoscience and Remote Sensing*, 29:16–20, 1991.

[11] M.O. Smith, J.B. Adams, and A.R. Gillepsie. Reference endmembers for spectral mixture analysis. *fifth Australian Remote Sensing Conference*, 1:331–340, 1990.

[12] C.J. Tucker. Red and photographic infrared linear combinations for monitoring vegetation. *Remote Sensing of Environment*, 8:127–150, 1979.